STEM CELLS®

TISSUE-SPECIFIC STEM CELLS

IFATS Collection: Fibroblast Growth Factor-2-Induced Hepatocyte Growth Factor Secretion by Adipose-Derived Stromal Cells Inhibits Postinjury Fibrogenesis Through a c-Jun N-Terminal Kinase-Dependent Mechanism

HIROTAKA SUGA,[a] HITOMI ETO,[a] TOMOKUNI SHIGEURA,[b] KEITA INOUE,[a] NORIYUKI AOI,[a] HARUNOSUKE KATO,[a] SATOSHI NISHIMURA,[c] ICHIRO MANABE,[d,e] KOICHI GONDA,[a] KOTARO YOSHIMURA[a]

Departments of [a]Plastic Surgery and [c]Cardiovascular Medicine and [d]Nano-Bioengineering Education Program, University of Tokyo, Tokyo, Japan; [b]Division of Research and Development, Biomaster Inc., Kanagawa, Japan; [e]PRESTO, Japan Science and Technology Agency, Tokyo, Japan

Key Words. Adipose-derived stem cells • Hepatocyte growth factor • Fibroblast growth factor-2 • c-Jun N-terminal kinase • Fibrogenesis • Ischemia-reperfusion injury

ABSTRACT

Adipose-derived stem/stromal cells (ASCs) not only function as tissue-specific progenitor cells but also are multipotent and secrete angiogenic growth factors, such as hepatocyte growth factor (HGF), under certain circumstances. However, the biological role and regulatory mechanism of this secretion have not been well studied. We focused on the role of ASCs in the process of adipose tissue injury and repair and found that among injury-associated growth factors, fibroblast growth factor-2 (FGF-2) strongly promoted ASC proliferation and HGF secretion through a c-Jun N-terminal kinase (JNK) signaling pathway. In a mouse model of ischemia-reperfusion injury of adipose tissue, regenerative changes following necrotic and apoptotic changes were seen for 2 weeks. Acute release of FGF-2 by injured adipose tissue was followed by upregulation of HGF. During the adipose tissue remodeling process, adipose-derived 5-bromo-2-deoxyuridine-positive cells were shown to be ASCs (CD31−CD34+). Inhibition of JNK signaling inhibited the activation of ASCs and delayed the remodeling process. In addition, inhibition of FGF-2 or JNK signaling prevented postinjury upregulation of HGF and led to increased fibrogenesis in the injured adipose tissue. Increased fibrogenesis also followed the administration of a neutralizing antibody against HGF. FGF-2 released from injured tissue acts through a JNK signaling pathway to stimulate ASCs to proliferate and secrete HGF, contributing to the regeneration of adipose tissue and suppression of fibrogenesis after injury. This study revealed a functional role for ASCs in the response to injury and provides new insight into the therapeutic potential of ASCs. STEM CELLS *2009;27:238–249*

Disclosure of potential conflicts of interest is found at the end of this article.

INTRODUCTION

Adipose-derived stem/stromal cells (ASCs) function as tissue-specific progenitor cells, can differentiate into cells of various lineages [1], and secrete many potent growth factors and cytokines, such as vascular endothelial growth factor (VEGF) and hepatocyte growth factor (HGF) [2–4]. Paracrine effects of the secreted factors account for improved vascularity of ischemic hind limbs treated with ASCs [2, 4]; however, ASC differentiation into endothelial cells could contribute to the improved vascularity as well [5, 6]. The use of ASCs for promoting angiogenesis and tissue repair has gained interest as a potential therapeutic strategy [7–9], and clinical trials involving ASC-mediated enhancement of bone and adipose regeneration and angiogenesis are under way [10–12].

ASCs not only secrete potent growth factors and cytokines but also are affected by them. Fibroblast growth factor-2 (FGF-2) stimulates the growth of ASCs [13, 14] and has been shown to promote adipogenic [15] and chondrogenic [13] differentiation of ASCs; however, FGF-2 inhibits their osteogenic differentiation [14]. Platelet-derived growth factor (PDGF) induces proliferation and migration of ASCs [16]. A culture medium containing VEGF, FGF-2, epidermal growth factor (EGF), and insulin-like growth factor-1 (IGF-1) markedly accelerated ASC proliferation and preserved their multipotency [17], suggesting synergism between these growth factors on ASC growth.

Mitogen-activated protein kinases (MAPKs) are important signal-transducing enzymes that are involved in many facets of cellular regulation by growth factors [18]. Among MAPKs, c-Jun N-terminal kinases (JNK) play key roles in PDGF-in-

Author contributions: H.S.: collection and/or assembly of data, data analysis and interpretation, manuscript writing; H.E., T.S., K.I., N.A., and H.K.: collection and/or assembly of data; S.N., I.M., and K.G.: data analysis and interpretation; K.Y.: conception and design, financial support, administrative support, collection and/or assembly of data, data analysis and interpretation, manuscript writing.

Correspondence: Kotaro Yoshimura, M.D., Department of Plastic Surgery, University of Tokyo School of Medicine, 7-3-1, Hongo, Bunkyo-Ku, Tokyo 113-8655, Japan. Telephone: 81-3-5800-8948; Fax: 81-3-5800-8947; e-mail: yoshimura-pla@h.u-tokyo.ac.jp Received March 20, 2008; accepted for publication August 28, 2008; first published online in STEM CELLS *EXPRESS* September 4, 2008. 1066-5099/2008/$30.00/0 doi: 10.1634/stemcells.2008-0261

duced proliferation and migration of ASCs [16]. There is also a study demonstrating that ASCs produce VEGF, HGF, and IGF-1 in response to tumor necrosis factor-α by a p38 MAPK-dependent mechanism [19].

In this study, we evaluated the influence of injury-associated growth factors on ASCs. In the process of injury and subsequent wound healing, various growth factors and inflammatory cytokines regulate regenerative cellular activities. We previously analyzed wound fluids after liposuction surgery and reported the sequential expression of growth factors; FGF-2 and PDGF were released in the early stage of wound healing, whereas VEGF and HGF were expressed in the later stage [20]. Administration of growth factors has been reported to enhance the regeneration of injured tissues, such as FGF-2 for burn [21] and HGF for myocardial infarction [22]. However, few studies have focused on the injury and repair process in adipose tissue and the potential role of ASCs, presumably because there is no good model of adipose tissue injury.

We hypothesized that ASCs stimulated by factors released from the injured tissue play an important role in the repair process of adipose tissue, perhaps by secreting regeneration-associated growth factors or by differentiating into adipocytes, endothelial cells, or other cell types. We examined the influence and mechanisms of injury-related factors on human and murine ASCs in vitro. Furthermore, using an original mouse model of ischemia-reperfusion injury to adipose tissue, we assessed the expression of injury-related growth factors at the cellular and molecular levels to elucidate the role of ASCs during the regeneration process.

Materials and Methods

Cell Isolation and Culture

Liposuction aspirates were obtained from healthy female donors (mean age, 35.4 ± 3.3; mean body mass index, 22.1 ± 1.2; $n = 9$) undergoing liposuction of the abdomen or thighs. Each patient provided her informed consent using an institutional review board-approved protocol prior to the procedure. ASCs were isolated from the aspirated fat as described previously [23]. Briefly, the aspirated fat was washed with phosphate-buffered saline (PBS) and digested on a shaker at 37°C in PBS containing 0.075% collagenase for 30 minutes. Mature adipocytes and connective tissue were separated from pellets by centrifugation (800*g*, 10 minutes). The cell pellets were resuspended, filtered through 100-μm mesh, plated at a density of 5×10^5 nucleated cells per 100-mm dish, and cultured at 37°C in an atmosphere of 5% CO_2 in humid air. The culture medium was Dulbecco's modified Eagle's medium (DMEM) containing 10% fetal bovine serum (FBS). Primary cells were cultured for 7 days and were defined as passage 0. The medium was replaced every 3 days. Cells were passaged every week by trypsinization. Human ASCs at passages 1–3 were used in the experiments. To separate mouse ASCs, adipose tissues were obtained from inguinal fat pads of 6-week-old male ICR mice. The adipose tissues were minced into 2–3-mm pieces and processed as described above. Mouse ASCs at passages 1–3 were used in the experiments. Human dermal fibroblasts (hDFs) were obtained from explant cultures of skin samples from separate donors; hDFs at passages 3–5 were used in the experiments. Human mesenchymal stem cells from bone marrow (hBM-MSCs), frozen at passage 2, were purchased from Cambrex (Walkersville, MD, http://www.cambrex.com); hBM-MSCs at passages 3–5 were used in the experiments.

Proliferation Assay

Human ASCs were plated in a six-well plate at 2×10^4 cells per well. Each injury-associated growth factor (VEGF, FGF-2, HGF, and PDGF; all from Wako Chemical, Osaka, Japan, http://www.wako-chem.co.jp/english) was added to the control medium (DMEM and 10% FBS) at concentrations of 0.1, 1, and 10 ng/ml. Cell number was counted after 3, 6, and 9 days in culture using a cell counter (NucleoCounter; ChemoMetec, Allerod, Denmark, http://www.chemometec.com). For other types of cells, 2×10^5 cells were plated in a 100-mm dish, and cell numbers were counted after 7 days. 5-Bromo-2-deoxyuridine (BrdU) incorporation assays were performed using the BrdU *In-Situ* Detection Kit (BD Biosciences, San Diego, http://www.bdbiosciences.com). Human ASCs were plated in a four-well chamber slide at 5×10^4 cells per well. Cells were cultured for 48 hours in control medium with a reduced serum concentration (2% FBS) with or without 10 ng/ml of various growth factors. Afterward, BrdU labeling was performed for 3 hours at a final concentration of 10 μM.

Flow Cytometry

Human ASCs cultured with VEGF, FGF-2, HGF, or PDGF at 10 ng/ml for 7 days were examined for surface marker expression using flow cytometry. The following fluorochrome-conjugated monoclonal antibodies were used: anti-CD31-phycoerythrin (PE), CD34-PE (BD Biosciences), Flk-1-PE, and Tie-2-PE (R&D Systems Inc., Minneapolis, http://www.rndsystems.com). Cells were incubated with each antibody for 30 minutes and then analyzed using an LSR II flow cytometry system (BD Biosciences). Gates were set on the basis of staining with combinations of relevant and irrelevant antibodies so that no more than 0.1% of cells were positive using irrelevant antibodies. Mouse stromal vascular fraction (SVF) cells were separated as described above, and multicolor flow cytometric analyses were performed using the following monoclonal antibodies conjugated to fluorochromes: anti-CD31-PE (BD Biosciences), CD34-fluorescein isothiocyanate (FITC) (eBioscience Inc., San Diego, http://www.ebioscience.com), CD45-PE Cy7 (Beckman Coulter, Fullerton, CA), APC BrdU Flow Kit (BD Biosciences), and Annexin V-FITC Apoptosis Detection Kit (BD Biosciences).

Quantitative Real-Time Reverse-Transcriptase Polymerase Chain Reaction

We isolated RNA from human ASCs cultured with VEGF, FGF-2, HGF, or PDGF at 10 ng/ml. For other types of cells, RNA was isolated from cells cultured with or without FGF-2 (10 ng/ml). We also isolated RNA from the inguinal adipose tissue of mouse models (described below) after homogenizing. Two micrograms of total RNA was isolated using an RNeasy Mini Kit (Qiagen, Hilden, Germany, http://www1.qiagen.com), followed by reverse transcription. We amplified cDNA for 40 cycles with the ABI 7700 (Applied Biosystems, Foster City, CA, http://www.appliedbiosystems.com) sequence detection system, a TaqMan Universal PCR Master Mix, and the following predesigned primers and fluorescein-labeled probes: human VEGF (Hs00900054_m1), FGF-2 (Hs00266645_m1), HGF (Hs00300159_m1), PDGF (Hs00234042_m1), glyceraldehyde-3-phosphate dehydrogenase (GAPDH) (Hs99999905_m1), mouse VEGF (Mm00437304_m1), FGF-2 (Mm00433287_m1), HGF (Mm01135182_m1), and GAPDH (Mm99999915_m1; all primers from Applied Biosystems). We calculated expression levels by the comparative C_T method using GAPDH as an endogenous reference gene.

Quantifying HGF Protein by Enzyme-Linked Immunosorbent Assay

Conditioned media of human ASCs cultured with or without FGF-2 (10 ng/ml) for 72 hours were analyzed by enzyme-linked immunosorbent assay (ELISA) using an ELISA kit for human HGF (Quantikine; R&D Systems). Data were expressed as the secreted factor per 10^6 cells at the time of harvest.

Inhibition of MAP Kinase Signaling Pathways

One selective inhibitor for each of three signaling pathways (extracellular signal-related kinase [ERK] inhibitor U0126, p38 protein inhibitor SB202190, and JNK inhibitor SP600125; all from Calbiochem, La Jolla, CA, http://www.emdbiosciences.com) was added at 10 μM with FGF-2 (10 ng/ml), and the effects on proliferation and gene expression were examined by proliferation assay and real-time reverse transcriptase-polymerase chain reaction (RT-PCR).

JNK Activity Assay

JNK activity was measured by the extent of c-Jun phosphorylation using a cell-based ELISA kit (CASE Kit; SuperArray Bioscience Corporation, Frederick, MD, http://www.superarray.com) according to the manufacturer's instructions. In brief, human ASCs were seeded at 2×10^4 per well in a 96-well plate and allowed to sit overnight. Cells were then starved in serum-free medium for 24 hours. Cells were pretreated with vehicle (0.1% dimethyl sulfoxide), U0126, SB202190, or SP600125 for 15 minutes, and then they were exposed to FGF-2 (10 ng/ml) or HGF (10 or 100 ng/ml) for 15 minutes. The amounts of activated (phosphorylated) c-Jun protein and total c-Jun protein were measured using anti-phospho-c-Jun (serine 73) antibody and anti-pan-c-Jun antibody.

Mouse Model for Ischemia-Reperfusion Injury to Adipose Tissue

Care of animals was in accordance with institutional guidelines. Six-week-old ICR mice were anesthetized with pentobarbital (50 mg/kg weight), and a 2-cm incision was made in the inguinal region. The subcutaneous inguinal fat pad was elevated, with the main nutrient vessels arising from the femoral vessels intact. Small communicating vessels to the skin from the fat pad were electrocoagulated. The main vessels were clamped with a vessel microclip for 3 hours and then released to allow reperfusion. The adipose tissue samples were harvested at various intervals (at days 1, 3, 7, and 14) after ischemia-reperfusion injury and examined by flow cytometry, real-time RT-PCR, Western blotting, and histology (hematoxylin-eosin staining, Azan staining, and others; described below). Fat samples from sham-operated animals (without ischemia-reperfusion injury) were used as controls. At each time point we confirmed that contralateral pads from experimental animals showed no pathological changes compared with the sham-operated animal samples (day 0 sample).

In Vivo Inhibition Assays

Inhibitor solutions were infused continuously using an osmotic pump (model 1007D; ALZET, Cupertino, CA, http://www.alzet.com) that released liquid at a rate of 0.5 μl/hour for approximately 7 days. The pump, containing 100 μl of a JNK inhibitor (SP600125; 10 μM), goat anti-FGF-2 antibody (50 μg/ml; R&D Systems), goat anti-mouse HGF antibody (50 μg/ml; R&D Systems), or control PBS, was implanted subcutaneously at the time of reperfusion.

Histological Detection of Apoptosis and Proliferation

To detect apoptosis after ischemia-reperfusion injury in adipose tissue, terminal deoxynucleotidyl transferase dUTP nick-end labeling (TUNEL) staining was performed using an *In-Situ* Cell Death Detection Kit (Roche Diagnostics, Mannheim, Germany, http://www.roche-applied-science.com). To detect proliferating cells, 1 mg of BrdU was administered intraperitoneally 6 and 3 hours before tissue harvest. BrdU-positive cells were detected using a BrdU *In-Situ* Detection Kit (BD Biosciences). The number of TUNEL- or BrdU-positive cells was counted at a ×200 magnification using three randomly selected fields per section.

Immunohistochemistry

Harvested adipose tissue samples were zinc-fixed (Zinc Fixative; BD Biosciences) and paraffin-embedded. We prepared 6-μm-thick sections and performed immunostaining using the following primary antibodies: goat anti-FGF-2 (R&D Systems), goat anti-mouse HGF (R&D Systems), goat anti-mouse CD68 (Santa Cruz Biotechnology Inc., Santa Cruz, CA, http://www.scbt.com), goat anti-mouse CD34 (Santa Cruz Biotechnology), rat anti-mouse CD31 (BD Biosciences), and biotinylated mouse anti-BrdU (BD Biosciences). For visualization with diaminobenzidine, peroxidase-conjugated secondary antibodies appropriate for each primary antibody (Nichirei, Tokyo, http://www.nichirei.co.jp/english/index.html) or a streptavidin-peroxidase complex (BD Biosciences) were used. For a double fluorescence staining, the following secondary antibodies and reagent were used: Alexa Fluor 488-conjugated rabbit anti-rat IgG, Alexa Fluor 488- or 568-conjugated donkey anti-goat IgG, and Alexa Fluor 568-conjugated streptavidin (Molecular Probes, Eugene, OR, http://probes.invitrogen.com). Isotypic antibody was used to serve as a negative control for each staining.

Western Blotting

Adipose tissue specimens were homogenized in 1 ml of lysis buffer (Santa Cruz Biotechnology) and centrifuged at 15,000 rpm for 2 minutes. The aqueous layer was collected and the protein concentration was determined using the bicinchoninate (BCA) protein assay kit (Pierce, Rockford, IL, http://www.piercenet.com). Equal amounts of protein (10 μg) were loaded into each lane of an SDS-polyacrylamide gel electrophoresis gel. The resolved proteins were transferred to a polyvinylidene difluoride membrane (Bio-Rad, Hercules, CA, http://www.bio-rad.com), and immunostaining was performed using goat anti-mouse FGF-2 antibody (R&D Systems), goat anti-mouse HGF antibody (R&D Systems), and goat anti-mouse GAPDH antibody (Santa Cruz Biotechnology). The GAPDH signal served as an internal control. Protein bands were quantified by volume summation of image pixels using Photoshop 7.0 (Adobe Systems Inc., San Jose, CA, http://www.adobe.com).

Glycerol-3-Phosphate Dehydrogenase Assay

A Glycerol-3-Phosphate Dehydrogenase (GPDH) Assay Kit (Primary Cell, Ishikari, Japan, http://www.primarycell.com) was used according to the manufacturer's instructions, as previously described [24]. In brief, each adipose tissue sample was mixed with a 0.25 M sucrose solution to a total of 5 ml, homogenized, and centrifuged. The supernatants were diluted 10 times with an enzyme-extracting reagent, and the optical absorption was measured at 340 nm for 10 minutes in a 96-well plate after addition of twice the volume of a substrate reagent. GPDH activity was calculated by the following formula: GPDH activity (U/ml) = $\Delta OD \times 0.482 \times 10$ (where ΔOD is change in optical density per minute).

Living Tissue Imaging

Visualization of living adipose tissue was performed using the procedure of Nishimura et al. [25]. Briefly, the adipose tissue was minced into 3-mm pieces and incubated with the following reagents for 30 minutes: BODIPY 558/568 or BODIPY-FL (both from Molecular Probes) to stain adipocytes, Alexa Fluor 488-conjugated isolectin GS-IB_4 (Molecular Probes) to stain endothelial cells, Hoechst 33342 (Dojindo, Kumamoto, Japan) to stain all nuclei, or propidium iodide (PI; Sigma-Aldrich, St. Louis, http://www.sigmaaldrich.com) to stain nuclei of necrotic cells. The sample was then washed and directly observed with a confocal microscope system (TCS SP2; Leica, Heerbrugg, Switzerland, http://www.leica.com).

Statistical Analysis

Results were expressed as mean ± SEM. Comparisons between two groups were performed with Welch's *t* test. Comparisons of multiple groups were done by analysis of variance with corrections for multiple comparisons. A value of $p < .05$ was considered significant.

RESULTS

Effects of Injury-Associated Growth Factors on Human ASC Proliferation

FGF-2 and PDGF promoted proliferation of human ASCs in a dose-dependent manner, whereas VEGF and HGF did not promote ASC growth (Fig. 1A). Morphologically, ASCs cultured with FGF-2 were smaller than ASCs cultured with other growth factors (Fig. 1B). The proliferative effects of FGF-2 and PDGF were also demonstrated in a BrdU incorporation assay. Cells were cultured in growth factor-containing medium with a reduced serum concentration (2% FBS) for a fixed period (48 hours) prior to assay (supporting information Fig. 1A).

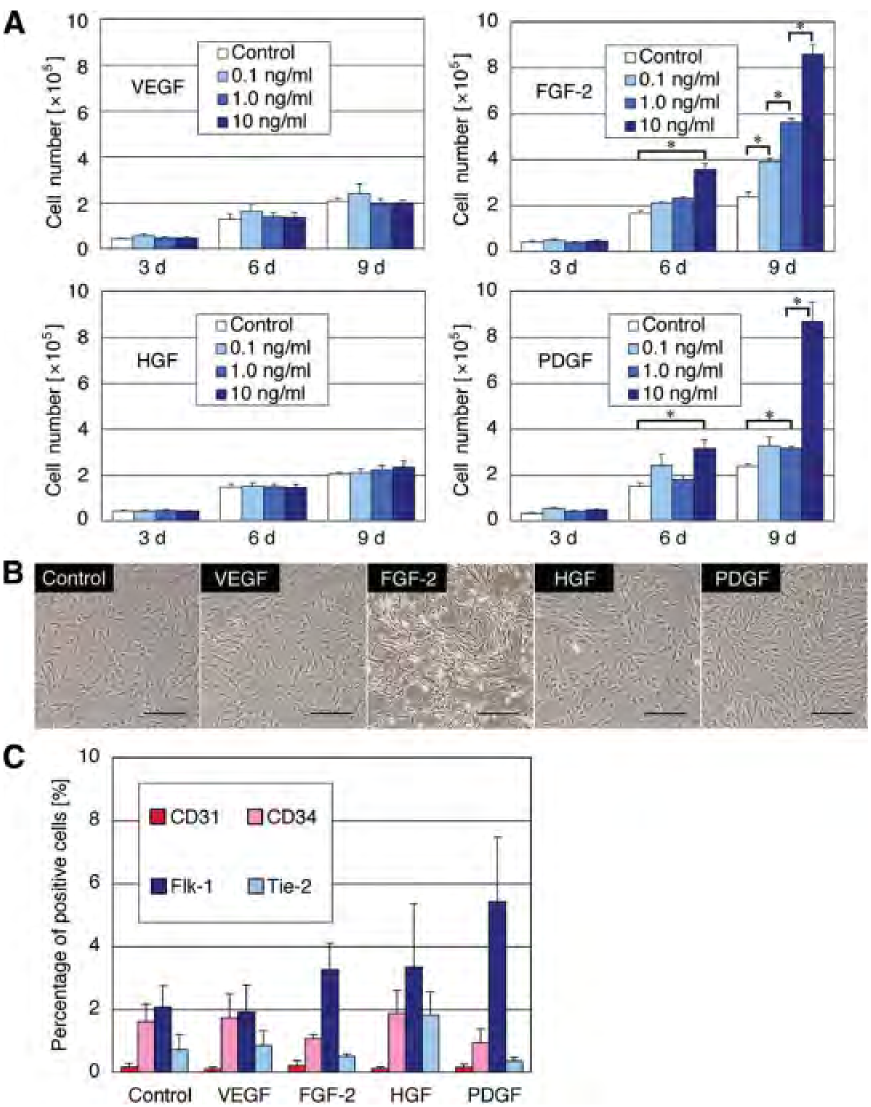

Figure 1. Effects of injury-associated growth factors on proliferation and surface marker expression of human adipose-derived stem/stromal cells (ASCs). **(A):** ASC counts after 3, 6, or 9 d of culture with VEGF, FGF-2, HGF, or PDGF. FGF-2 and PDGF promoted proliferation of human ASCs in a dose-dependent manner, whereas VEGF and HGF showed no proliferative effects ($n = 4$; $*$, $p < .05$). **(B):** Light microscopy photographs of human ASCs cultured with each growth factor for 6 d. Cells cultured with FGF-2 (10 ng/ml) were smaller than those cultured with other growth factors. Scale bars = 200 μm. **(C):** Flow cytometric analyses of human ASCs cultured with each growth factor for 7 d. No significant changes in the expression of vascular endothelial markers (CD31, CD34, Flk-1, and Tie-2) were observed. Abbreviations: d, day; FGF, fibroblast growth factor; HGF, hepatocyte growth factor; PDGF, platelet-derived growth factor; VEGF, vascular endothelial growth factor.

Phenotypic Effects of Injury-Associated Growth Factors on Human ASCs

Flow cytometry showed no significant changes in expressions of endothelial surface markers (CD31, CD34, Flk-1, and Tie-2) by any injury-associated growth factors, indicating that supplementation of a single factor is not enough to induce endothelial differentiation of human ASCs, at least when cultured without any extracellular matrices (Fig. 1C; supporting information Fig. 1B).

Interactive Effects of Injury-Associated Growth Factors on Their Expressions by Human ASCs

FGF-2 and PDGF significantly downregulated expression of their own transcripts by human ASCs, and FGF-2 also significantly suppressed PDGF mRNA expression (Fig. 2A). Most interestingly, FGF-2 promoted a striking increase in HGF mRNA expression. Time course evaluation revealed that the upregulation of HGF mRNA was biphasic, with the first peak at 6 hours and a striking increase beginning after 24 hours (Fig. 2B). ELISA of culture media demonstrated that HGF protein secretion by FGF-2-stimulated human ASCs was significantly elevated at day 3 (Fig. 2C).

Intracellular Signaling Pathways of FGF-2-Induced Effects on Human ASCs

The proliferative effects of FGF-2 on human ASCs were significantly inhibited by a JNK inhibitor (SP600125) but not by an ERK inhibitor (U0126) or a p38 inhibitor (SB202190; Fig. 3A). Upregulation of HGF mRNA by FGF-2 was also significantly inhibited by the JNK inhibitor (Fig. 3B). Administration of the ERK and p38 inhibitors slightly decreased the expression level of HGF mRNA, although the changes were not statistically significant, suggesting crosstalk between JNK and other signaling pathways. Phosphorylation of c-Jun, the prototypical nuclear effector of the JNK signal transduction pathway, increased with FGF-2 treatment, and the FGF-2-induced upregulation of c-Jun phosphorylation was completely prevented by pretreatment with the JNK inhibitor (Fig. 3C). On the other hand, HGF did not increase phosphorylation of c-Jun in human ASCs (Fig. 3C). These results indicate that FGF-2 promotes proliferation and HGF mRNA expression predominantly through the JNK signaling pathway.

FGF-2-Induced Effects in Human ASCs and Other Cell Types

Cell growth was promoted by FGF-2 in all four cell types studied (human ASCs, human dermal fibroblasts [DFs], human

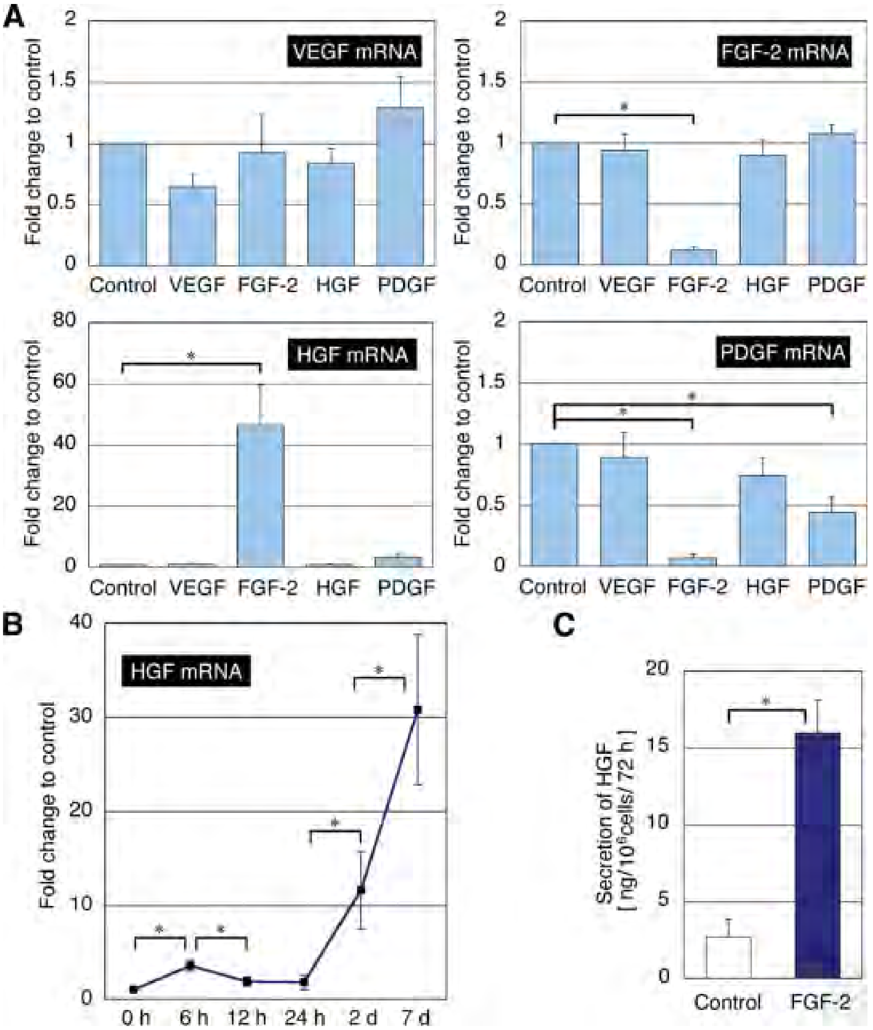

Figure 2. Interactive effects of injury-associated growth factors on their own mRNA expression by human adipose-derived stem/stromal cells (ASCs). **(A):** Injury-associated growth factor mRNA expression by human ASCs. FGF-2 (10 ng/ml) induced striking upregulation of HGF mRNA expression by human ASCs, whereas FGF-2 and PDGF downregulated their own expression ($n = 7$; *, $p < .05$). **(B):** Time course of HGF mRNA expression induced by FGF-2. FGF-2 (10 ng/ml) promoted biphasic HGF mRNA expression by human ASCs, with the first peak occurring at 6 h and the second increase beginning after 24 h ($n = 6$; *, $p < .05$). **(C):** FGF-2-induced HGF protein secretion by human ASCs. Enzyme-linked immunosorbent assay of cultured media on d 7 showed that FGF-2 (10 ng/ml) promoted secretion of HGF protein from human ASCs ($n = 4$; *, $p < .05$). Abbreviations: d, day; FGF, fibroblast growth factor; h, hour; HGF, hepatocyte growth factor; PDGF, platelet-derived growth factor; VEGF, vascular endothelial growth factor.

mesenchymal stem cells from bone marrow [BM-MSCs], and murine ASCs), although the basal proliferative capacity differed among cell types. The FGF-2-enhanced cell proliferation was significantly inhibited by a JNK inhibitor (SP600125) in all cell types examined (Fig. 3D). HGF mRNA expression was also promoted by FGF-2 in all cell types, and the upregulation of HGF mRNA was significantly inhibited by the JNK inhibitor except in human BM-MSCs (Fig. 3E), suggesting that HGF mRNA upregulation by FGF-2 was mediated through signaling pathways other than JNK in human BM-MSCs.

Ischemia-Reperfusion Injury and Subsequent Repair in the Inguinal Adipose Tissue of Mice

The murine inguinal fat pad consistently had a dominant feeding artery and vein without anatomical anomaly, which enabled reproducible ischemia-reperfusion injury experiments (Fig. 4A). The weight of the adipose tissue was increased on day 1, suggesting tissue edema (supporting information Fig. 2A), whereas GPDH activity, which correlates with the total number and size of mature adipocytes, did not change significantly during the experimental period (supporting information Fig. 2B). Histologically, interstitial infiltration of blood cells was observed as early as day 1 and was most prominent on day 3. Small adipocytes appeared on day 1 and increased in number on day 3, suggesting that lipolysis or adipogenesis took place throughout the adipose tissue. On day 7, infiltrated erythrocytes disappeared and some adipocytes increased in size, whereas a substantial number of nucleated cells remained in the interstitial space between adipocytes (Fig. 4B). Flow cytometric analysis of the SVF showed that the total number of SVF cells, as well as the number of CD45+ cells, was increased by day 7, whereas the number of CD34+/CD31− cells peaked on day 3 (Fig. 4C). The number of BrdU-positive proliferating cells increased from day 1 and peaked on day 3 (Fig. 4D; supporting information Fig. 2C), and most BrdU+/CD45− cells (88.2% ± 4.2%; $n = 3$) were shown to be CD34+/CD31− (Fig. 4E). The frequency of TUNEL-positive apoptotic cells was significantly high (6%–9% of nucleated cells) on day 1 and decreased thereafter (Fig. 4F; supporting information Fig. 2D). Flow cytometry demonstrated that most Annexin V-positive apoptotic cells on day 1 (90.1% ± 3.0%; $n = 3$) were CD45+ (Fig. 4G). In addition, an increase in PI-positive necrotizing cells was observed on day 3; some of these cells (17.2% ± 5.5%; $n = 3$) were lectin-positive, suggesting that some capillary endothelial cells were necrotizing and that capillary remodeling was under way (Fig. 4H). These results indicate that the adipose tissue was impaired soon after reperfusion, apoptosis and necrosis were involved in the process of adipose degeneration, and regenerative changes occurred thereafter.

FGF-2 protein was detected in the interstitial tissue by immunohistochemistry as early as day 1, with a peak of detection on day 3, although not much FGF-2 was expressed on day 7 (Fig. 5A). Western blotting also showed an increase in FGF-2 protein on days 1 and 3 (Fig. 5B). On the other hand, little HGF

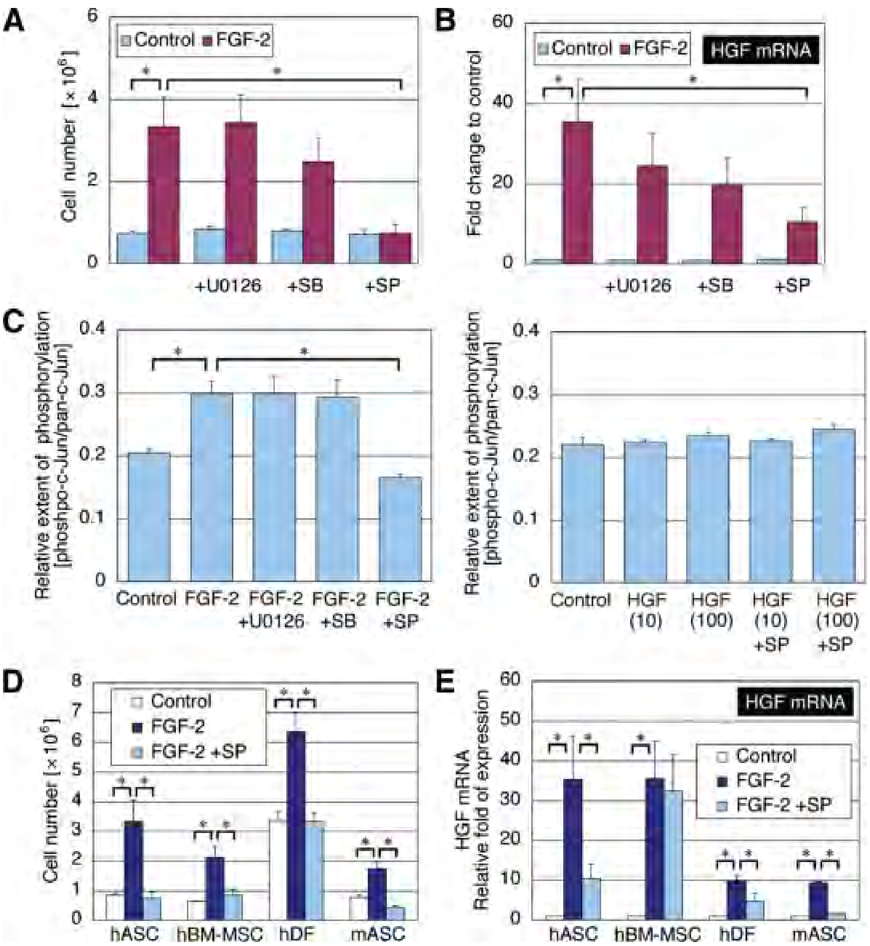

Figure 3. Inhibition of FGF-2 intracellular signaling pathways. **(A):** Effects of downstream signal inhibitors on adipose-derived stem/stromal cell (ASC) counts after 7 days in culture with or without FGF-2 (10 ng/ml). The JNK inhibitor SP significantly inhibited the proliferative effect of FGF-2 on hASCs, whereas U0126 (an ERK inhibitor) and SB (a p38 protein inhibitor) showed no or limited inhibitory effect on ASC proliferation ($n = 5$; $*$, $p < .05$). **(B):** HGF mRNA expression by human ASCs cultured with or without FGF-2 (10 ng/ml) on day 7. FGF-2-induced upregulation of HGF mRNA was significantly inhibited by SP ($n = 5$; $*$, $p < .05$), whereas U0126 and SB had limited inhibitory effects. **(C):** Inhibitor specificity. Left: Phosphorylation of c-Jun increased following 15-minute treatment with FGF-2 (10 ng/ml). FGF-2-induced phosphorylation of c-Jun was completely prevented by pretreatment with SP ($n = 4$; $*$, $p < .05$). Right: Phosphorylation of c-Jun increased with HGF treatment (10 or 100 ng/ml). HGF, even at a high concentration (100 ng/ml), did not increase c-Jun phosphorylation in hASCs ($n = 3$). **(D):** Cell counts after 7 days in culture. FGF-2-induced cell proliferation was significantly inhibited by the JNK inhibitor SP in all cell types examined (hASCs, hBM-MSCs, hDF, mASC; $n = 5$; $*$, $p < .05$). **(E):** Real-time polymerase chain reaction assays for HGF mRNA expression on day 7. HGF mRNA expression was promoted by FGF-2 in all cell types, whereas the FGF-2-induced upregulation of HGF mRNA was significantly inhibited by a JNK inhibitor except in hBM-MSCs ($n = 5$; $*$, $p < .05$). Abbreviations: FGF, fibroblast growth factor; hASC, human adipose-derived stem/stromal cell; hBM-MSC, human bone marrow-derived mesenchymal stem cell; hDF, human dermal fibroblasts; HGF, hepatocyte growth factor; mASC, mouse adipose-derived stem/stromal cell; SB, SB202190; SP, SP600125.

protein was detected on day 1, but HGF expression was elevated from day 3 until at least day 7 (Fig. 5C, 5D). Interestingly, FGF-2 mRNA was downregulated from soon after injury throughout the 2 weeks, suggesting that FGF-2 was released from the storage of the injured adipose tissue, such as extracellular matrix or dying cells, rather than produced by viable cells such as ASCs. The released FGF-2 might downregulate FGF-2 mRNA expression by ASCs in the injured adipose tissue, as was seen in human ASCs in vitro. In contrast, HGF mRNA expression in the tissue was significantly elevated on day 3, but not on days 1 and 7 (Fig. 5E), suggesting that the delayed upregulation of HGF mRNA and secretion of HGF were likely induced by the preceding release of FGF-2 protein. Thus, the data suggest that FGF-2 is provided temporarily only when an event such as injury occurs and triggers FGF-JNK-HGF signaling, thereby promoting repair processes such as angiogenesis.

Cellular Events in the Repair Process of Injured Adipose Tissue

Before injury, CD34+/CD31− cells, which were regarded as ASCs, were found throughout the intact adipose tissue, located between mature adipocytes, and were especially abundant around vessels (supporting information Fig. 3A). The number of CD34+/CD31− cells was apparently much larger than that of CD31+ endothelial cells, which were negative or faintly positive for CD34. Most BrdU-positive proliferating cells, frequently detected 3 days after injury, were also positive for CD34 (Fig. 6A, top), and most CD34+ cells were lectin-negative (Fig. 6A, bottom), which suggests that CD34+/lectin− ASCs play substantial roles in the repair process. Living tissue imaging revealed increases in interstitial space and in the number of small adipocytes (less than 50 μm in diameter); an increase in the number of nucleated cells, including lectin-positive round cells (Fig. 6B); and an increase in the number of capillaries, especially around small adipocytes (supporting information Fig. 3B). On day 7, large adipocytes were not seen in samples treated with a JNK inhibitor, whereas large adipocytes were seen in untreated models (Fig. 6B, 6C). Furthermore, PI-positive nuclei were frequently observed on days 1 and 3, a small number of which (10.7% ± 5.7% on day 1; 4.4% ± 0.5% on day 3; $n = 3$) were seen in adipocytes, suggesting that not only capillary endothelial cells (Fig. 4H) but also adipocytes were necrotizing (Fig. 6D). On day 7, the PI-positive nuclei were still observed in samples treated with a JNK inhibitor, although they were rarely detected in untreated models (Fig. 6D, 6E). These results suggest that the adipose tissue remodeling involving adipocytes and capillaries was under way during the 1st week after injury and the tissue repair process was impaired by treatment with a JNK inhibitor. CD68+ cells, regarded as infiltrating macrophages, were scarcely detected in the intact adipose tissue (supporting information Fig. 3C). However, infiltrated macrophages aggregated around small adipocyte-like cells after injury, suggesting

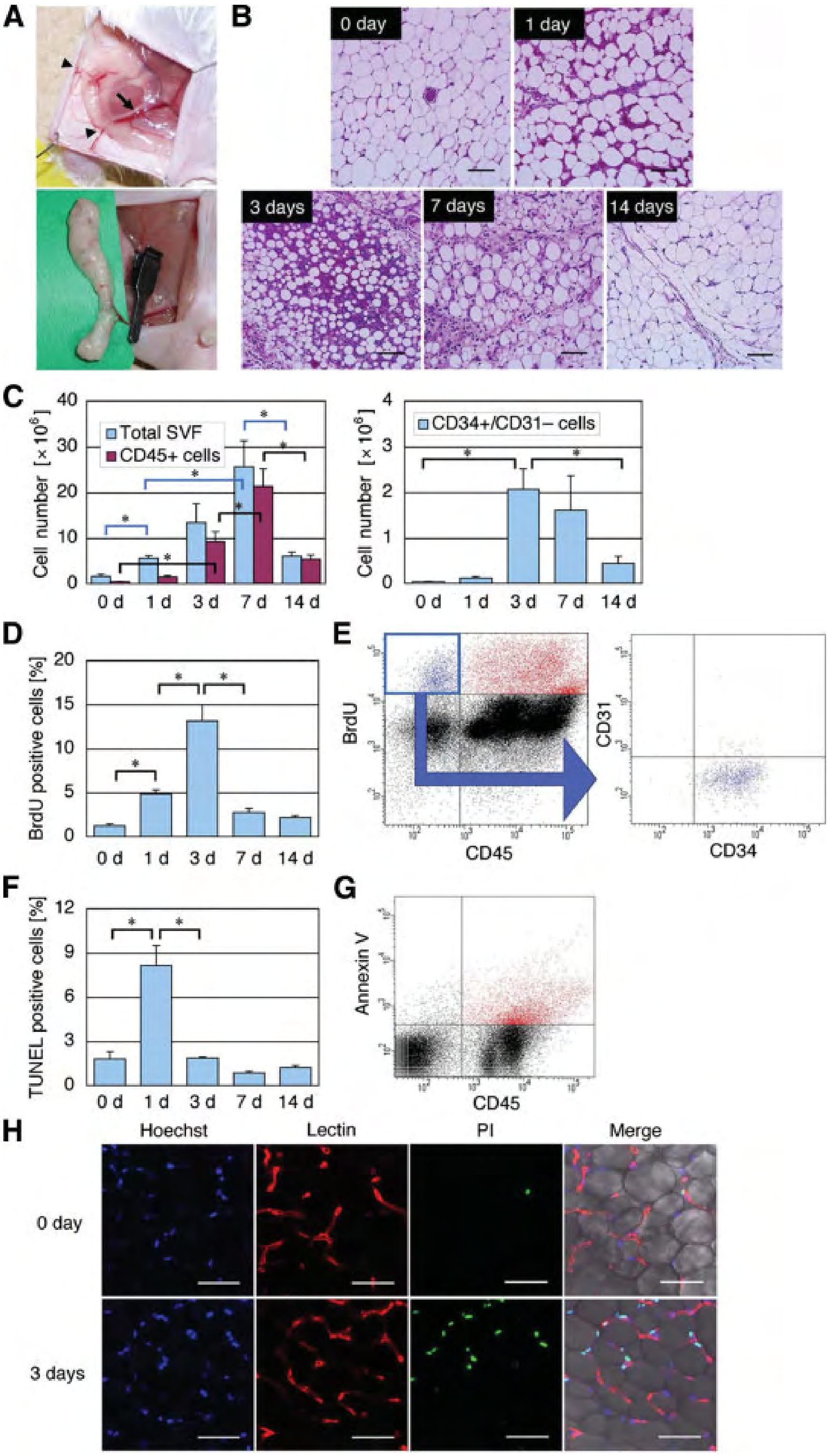

Figure 4. Ischemia-reperfusion injury and subsequent regenerative changes in the inguinal adipose tissue of mice. **(A):** Ischemia-reperfusion injury model. Top: The murine inguinal fat pad. The arrow indicates the dominant nutrient vessels arising from the femoral vessels. Arrowheads indicate communicating branches to the skin. Bottom: The communicating branches were severed, and the dominant vessels were clamped for 3 hours with a vessel clip. **(B):** Hematoxylin-eosin staining revealed that interstitial infiltration of blood cells occurred as early as d 1 and diminished by d 7. Regenerative changes were seen in the injured adipose tissue throughout the 1st week. Scale bars = 100 μm. **(C):** Analysis of SVF by flow cytometry. Left: Total SVF cells and CD45+ cells. Right: CD31−/CD34+ cells. Total SVF cells increased by d 7, with the similar increase of CD45+ cells, whereas the number of CD34+/CD31− cells peaked on d 3 ($n = 3$; ∗, $p < .05$). **(D):** Quantification of BrdU-positive cells by immunohistochemistry (supporting information Fig. 2C). BrdU-positive proliferating cells increased after injury, peaking on d 3 ($n = 4$; ∗, $p < .05$). **(E):** Flow cytometric analysis of SVF cells on d 3. BrdU-positive proliferating cells included both CD45+ and CD45− cells; most BrdU+/CD45− cells (88.2% ± 4.2%; $n = 3$) were CD34+/CD31−. **(F):** Quantification of TUNEL-positive cells by immunohistochemistry (supporting information Fig. 2D). TUNEL-positive apoptotic cells were observed most frequently 1 d after injury ($n = 4$; ∗, $p < .05$). **(G):** Flow cytometric analysis of SVF cells for expression of Annexin V and CD45 on d 1. Most Annexin V-positive apoptotic cells (90.1% ± 3.0%; $n = 3$) were CD45+. **(H):** Living tissue stained with Hoechst 33342 (blue), lectin (endothelial cells; red), or PI (necrotic cells; green), imaged and merged with interference contrast images. PI-positive necrotizing cells increased on d 3; some of these cells (17.2% ± 5.5%; $n = 3$) appeared to be lectin-positive capillary endothelial cells. Scale bars = 100 μm. Abbreviations: BrdU, 5-bromo-2-deoxyuridine; d, day; PI, propidium iodide; SVF, stromal vascular fraction; TUNEL, terminal deoxynucleotidyl transferase dUTP nick-end labeling.

phagocytosis. This aggregation of CD68+ cells was most frequently observed 3 days after injury.

Influence of Signal Inhibition on HGF Expression and Fibrogenesis After Ischemia-Reperfusion Injury

The increase in BrdU-positive proliferating cells on day 3 was significantly inhibited by treatment with a JNK inhibitor or a neutralizing antibody against FGF-2 but not by a neutralizing antibody against HGF (Fig. 7A). Immunohistochemical analysis demonstrated that the JNK inhibitor also suppressed the number of CD34+/lectin− ASCs on days 3 and 7 (supporting information Fig. 3D). Administering a JNK inhibitor or a neutralizing antibody against FGF-2 completely prevented upregulation of HGF mRNA in the injured adipose tissue on day 3 (Fig. 7B) and suppressed HGF secretion on day 7 (Fig. 7C, 7D). Histological measurement of the fibrous area at 2 weeks revealed that reper-

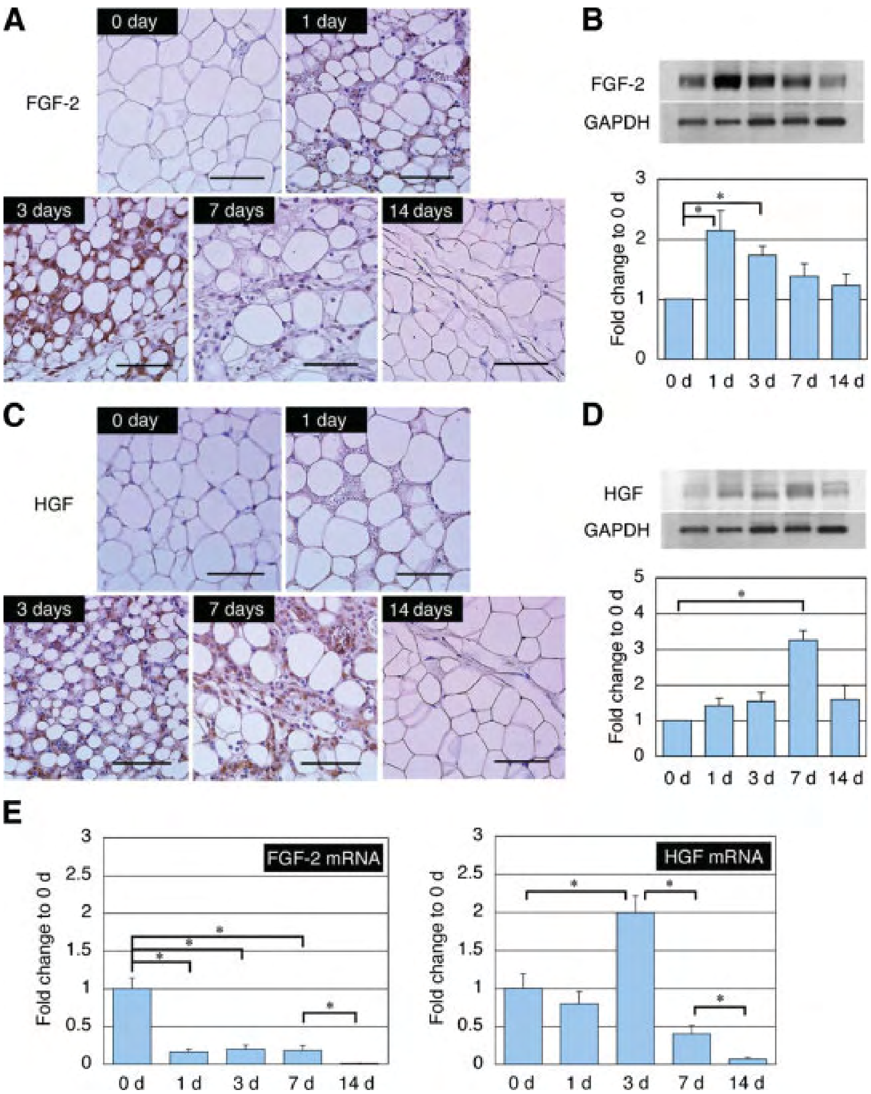

Figure 5. Expression of FGF-2 and HGF after ischemia-reperfusion injury to the adipose tissue. **(A):** Immunostaining for FGF-2. FGF-2 protein was detected as early as 1 d postinjury, with the peak of detection on d 3. Scale bars = 100 μm. **(B):** Western blot analysis for FGF-2. FGF-2 protein increased significantly on d 1 and 3 (n = 3; $*$, $p < .05$). **(C):** Immunostaining for HGF. Little HGF protein was detected 1 d after injury, but it was detected as late as 3 d postinjury, peaking 7 d after injury. Scale bars = 100 μm. **(D):** Western blot analysis for HGF. HGF protein increased significantly on d 7 (n = 3; $*$, $p < .05$). **(E):** Real-time polymerase chain reaction assay of FGF-2 mRNA and HGF mRNA expressions in the injured adipose tissue. FGF-2 mRNA was downregulated soon after injury (n = 5; $*$, $p < .05$), whereas HGF mRNA was significantly upregulated 3 d after injury (n = 5; $*$, $p < .05$). Abbreviations: d, day; FGF, fibroblast growth factor; GAPDH, glyceraldehyde-3-phosphate dehydrogenase; HGF, hepatocyte growth factor.

fusion injury to the adipose tissue caused a significant increase in the fibrous area (from 10% to 23%). Furthermore, inhibition of JNK or FGF-2 signaling caused a further significant increase in the fibrous area compared with administration of vehicle alone. Significantly increased fibrogenesis was also observed in the group treated with an anti-HGF antibody (Fig. 7E). These results indicated that fibrogenesis seen in the injured adipose tissue was suppressed by HGF in the process of adipose tissue repair and suggested that HGF secretion, mainly from ASCs, was induced by FGF-2 through a JNK signaling pathway.

Discussion

After mechanical injury to human adipose tissue, FGF-2, EGF, transforming growth factor (TGF)-β, and PDGF are first secreted in the early stage of wound healing. Thereafter, as the above growth factors decline, VEGF and HGF secretion gradually increases during the 1st week postinjury [20]. Our results indicated that among these injury-associated growth factors, FGF-2 promoted proliferation and HGF secretion by ASCs predominantly through a JNK signaling pathway. FGF-2 is an important endogenous stimulator of angiogenesis [26] and cell proliferation [27] and is known to be released during the early phase of wound healing [28, 29]. Cellular FGF-2 is released during the lysis of various cell types, such as fibroblasts [30] and endothelial cells [31], around the wound, whereas FGF-2 bound up in the extracellular matrix is released by the action of various wound proteases [32, 33]. JNK signaling is involved not only in FGF-2-induced ASC proliferation, as revealed in this study, but also in PDGF-induced proliferation and migration of human ASCs [16]. Therefore, it is likely that the JNK inhibitor used in this study inhibited the biological action of both FGF-2 and PDGF on ASCs. PDGF promoted ASC proliferation but had no significant effect on HGF expression by ASCs. As other researchers have reported, both FGF-2 and EGF promoted HGF secretion by ASCs [3]; therefore, JNK might also be involved in the EGF-induced HGF secretion by ASCs. Although some studies using other cell types found that JNK was involved in the HGF signaling pathway [34, 35], our results indicated that HGF, even at high concentrations, did not stimulate the JNK pathway in human ASCs.

It is interesting that the FGF-2-enhanced cell proliferation and HGF production that we observed for ASCs were observed also in other mesenchymal cell types, such as BM-MSCs and DFs, although HGF mRNA upregulation in human BM-MSCs was mediated by signals other than JNK. FGF-2-induced HGF upregulation has been observed in other cell types, such as smooth muscle cells [36], fibroblast-like cells from lung tissue

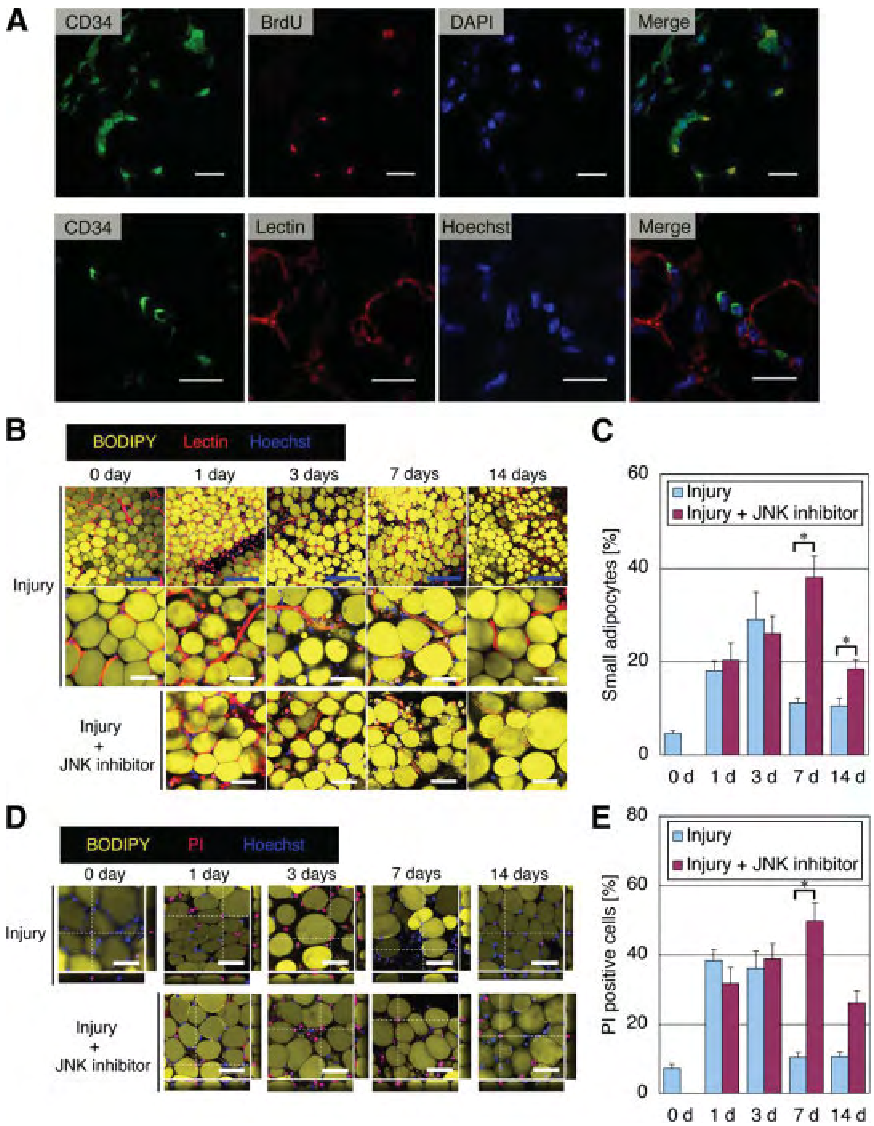

Figure 6. Cellular events in the repair process of injured adipose tissue. **(A):** The injured tissue on d 3. Top: Staining for CD34 (green), BrdU (red), and Hoechst 33342 (blue). Most BrdU-positive cells, frequently observed 3 d after injury, were also positive for CD34. Scale bars = 20 μm. Bottom: Living tissue image of the tissue on d 3 stained with CD34 (green), lectin (endothelial cells; red), and Hoechst 33342 (nuclei; blue). On d 3, most of CD34+ cells were lectin-negative, suggesting that they were adipose-derived stem/stromal cells. Scale bars = 20 μm. **(B):** Living tissue image stained with BODIPY (adipocytes; yellow), lectin (endothelial cells; red), and Hoechst 33342 (nuclei; blue). Increased numbers of nucleated cells and small adipocytes were observed on d 1 and d 3. Lectin+ small round cells, which may be infiltrating blood-derived cells, were seen on d 1, although they remained to be characterized. Large adipocytes increased on d 7, but not when treated with a JNK inhibitor. Blue scale bars = 200 μm; white scale bars = 50 μm. **(C):** Quantification of small adipocytes (less than 50 μm in diameter). In the group treated with a JNK inhibitor, the percentages of small adipocytes were significantly higher on d 7 and 14 ($n = 3$; $*$, $p < .05$). **(D):** Three-dimensional images of living tissue stained with BODIPY (adipocytes; yellow), PI (nuclei of necrotizing cells; red), and Hoechst 33342 (all nuclei; blue); images dissected horizontally and longitudinally at levels of white broken lines are also shown. PI-positive cells were frequently observed on d 1 and 3; some of these cells (10.7% $\pm$ 5.7% on d 1; 4.4% $\pm$ 0.5% on d 3; $n = 3$) were proven to be adipocytes. Treatment with a JNK inhibitor increased the number of PI-positive cells on d 7. Scale bars = 50 μm. **(E):** Quantification of PI-positive cells. In the group treated with a JNK inhibitor, the percentage of PI-positive cells was significantly higher on d 7 ($n = 3$; $*$, $p < .05$). Abbreviations: BrdU, 5-bromo-2-deoxyuridine; d, day; DAPI, 4,6-diamidino-2-phenylindole; JNK, c-Jun N-terminal kinase; PI, propidium iodide.

[37], and osteoblasts [38]; however, the intracellular signaling mechanisms were not well investigated. Other factors, such as interleukin-1 [39], interferon-γ [40], and ascorbic acid [41], have also been reported to stimulate HGF production. HGF is a key mediator of angiogenesis and wound healing, and its expression seems to be regulated by a number of factors in various cells and tissues.

The injury and repair process in adipose tissue has not been well studied, presumably because there is no standard animal model. Coban et al., using the epigastric adipo-cutaneous flap model, described edema and hemorrhage following ischemia-reperfusion injury of adipose tissue [42]; their results were similar to ours, even though a different model was used. In the injured adipose-tissue, necrotic and apoptotic changes followed edema and hemorrhage in the early phase after injury, and inflammatory and regenerative changes, such as phagocytosis, cell infiltration and proliferation, were observed throughout the 1st week. The necrotic changes were seen in capillary endothelial cells and adipocytes, suggesting adipose tissue remodeling, the repair process of which was impaired by a JNK inhibitor. HGF secretion followed release of FGF-2, stored bound or in other forms, from the tissue; the HGF upregulation appears to be derived predominantly from ASCs stimulated by FGF-2 via JNK signaling pathway, because ASCs are known to constitute more than one-half of the mesenchymal cells in stromal vascular fractions derived from adipose tissue [23]. The ischemia-reperfusion model used in this study provided reproducible results of injury and regeneration of adipose tissue, all of which were complete within 2 weeks.

In the adipose tissue, CD34+/CD31− cells, which were suggested to be ASCs, were seen in abundance between adipocytes (closely related to capillaries) and around vessel walls (especially in the tunica adventitia) before injury. CD34+ vascular wall resident progenitor cells, which have the capacity to differentiate into vascular endothelial cells and form capillary sprouts, were previously reported [43], and this population might constitute part of ASCs. On the other hand, a periendothelial subpopulation of ASCs with pericytic characteristics has been also characterized [44]. ASCs might consist of heterogenic subpopulations, which may explain the complexity in elucidating ASC characteristics and functions in vivo. As previously suggested, there is a close relationship between adipogenesis

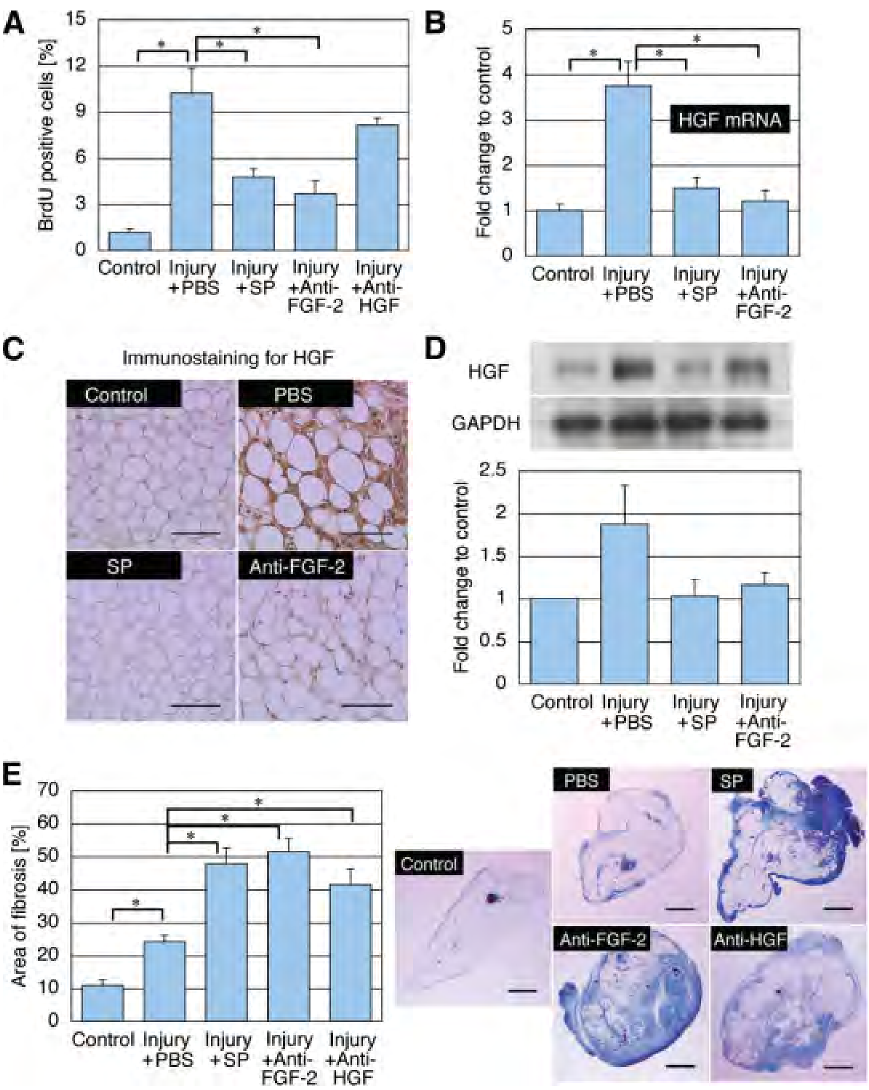

Figure 7. Influences of signal inhibition after ischemia-reperfusion injury to adipose tissue. **(A):** Proliferating cell counts according to immunohistology on day 3. The injury-induced increase in BrdU-positive proliferating cells was significantly inhibited by a JNK inhibitor (SP) or an anti-FGF-2 antibody (n = 4; *, $p < .05$) but not by an anti-HGF antibody. **(B):** HGF mRNA expression by adipose tissue on day 3. Continuous administration of SP or anti-FGF-2 antibody prevented upregulation of HGF mRNA on day 3 (n = 5; *, $p < .05$). **(C):** Immunostaining for HGF on day 7. Continuous administration of SP or anti-FGF-2 antibody inhibited HGF secretion in the injured adipose tissue on day 7. Scale bars = 100 μm. **(D):** Western blot analysis for HGF on day 7. Treatment with SP and anti-FGF-2 antibody inhibited the expression of HGF protein. **(E):** Fibrogenesis in the injured adipose tissue at 2 weeks after injury. Fibrotic area was stained with Azan staining. Scale bar = 1 mm. Ischemia-reperfusion injury induced significant fibrogenesis; the area of fibrosis was twice as large as that in the uninjured animal. Continuous administration of SP, anti-FGF-2, or anti-HGF antibody significantly increased fibrosis (n = 6; *, $p < .05$). Abbreviations: BrdU, 5-bromo-2-deoxyuridine; FGF, fibroblast growth factor; GAPDH, glyceraldehyde-3-phosphate dehydrogenase; HGF, hepatocyte growth factor; PBS, phosphate-buffered saline; SP, SP600125.

and angiogenesis; therefore, ASCs, which are primarily regarded as adipocyte progenitor cells, may function as adipogenic and angiogenic progenitors [5] and manage the interplay of adipocytes, blood cells, and blood vessels in various situations, such as obesity [25], adipose tissue turnover, and postinjury adipose tissue repair. During tissue regeneration, more CD34+/CD31− ASCs were found between adipocytes than in controls, and most BrdU-positive proliferating cells seen on day 3 were CD34+/lectin−, suggesting that ASCs are proliferating and participating in repair processes such as adipogenesis and angiogenesis. The proliferation and migration of ASCs were strongly inhibited by treatment of a JNK inhibitor, resulting in delayed and impaired tissue repair as well as increased fibrogenesis. Macrophages are known to be involved in inflammation in adipose tissue and obesity [25]. In this study, CD68+ macrophages were scarcely detected in controls but were seen in larger numbers on day 3, though at a much lower level than in ASCs. The role of macrophages in the injured adipose tissue remains to be clarified, but they may be involved in phagocytosis and/or angiogenesis [25].

HGF has been reported to have antifibrogenic effects in various organs, including heart [22], liver [45], and kidney [46]. Recent studies have revealed that HGF antagonizes the profibrotic actions of TGF-β by intercepting Smad signal transduction through diverse mechanisms [46, 47]. In this study, inhibiting FGF-2 signaling suppressed HGF production by ASCs, and inhibition of HGF led to increased fibrogenesis in the injured adipose tissue. Furthermore, administering a JNK inhibitor or an anti-FGF-2 antibody also resulted in severe postinjury fibrogenesis, which means that FGF-2-induced prevention of fibrogenesis was mediated at least in part by HGF derived from ASCs and that HGF is a key factor in preventing fibrogenesis and preserving adipose volume after injury. FGF-2 is known to promote wound healing by its direct effects on fibroblasts and endothelial cells [48], but this study revealed that FGF-2 could also promote tissue repair and prevent fibrogenesis by inducing HGF from ASCs and/or DFs. Because adipose tissue exists in or around most organs, FGF-2-induced HGF secretion from ASCs might be important in the repair processes following organ injuries such as myocardial infarction, hepatitis, and nephritis.

The results of this study provide new insights into the therapeutic potential of ASCs. Cytotherapies with ASCs, especially when pretreated or combined with FGF-2, might accelerate tissue repair, reduce fibrosis, and improve the function of organs impaired by acute or chronic inflammation through HGF action. It has been suggested that HGF secreted by ASCs might play an important role in autologous fat grafting [9, 12], promoting adipose graft survival and preventing scar formation. HGF is not only antifibrogenic but also angiogenic [49], and it has been shown to contribute to angiogenesis in adipose tissue [50] and to the improvement of ischemic limb [51]. FGF-2-induced HGF secretion could also promote angiogenesis during tissue repair. The total capillary amount was increased, but the vascular density in the injured adipose tissue was not (supporting information Fig. 3E), although the measured value (of vascular density) can be affected by the size and density of adipocytes. In ASCs, VEGF secretion appears to be induced by hypoxia [2]. The model we used in this study was an injury model rather than an ischemia model, and VEGF expression was downregulated soon after injury (data not shown). To study angiogenesis in adipose tissue and establish a therapeutic strategy for enhancing angiogenesis, studies using specific models of chronic ischemia in adipose tissue are needed.

Conclusion

FGF-2 promotes proliferation of and HGF secretion by ASCs through a JNK signaling pathway. In injured adipose tissue, ASCs stimulated by FGF-2 released from injured tissue are suggested to be the main proliferating cell population in the adipose repair process. This JNK-mediated signal plays an important role in preventing fibrogenesis and preserving adipose volume after injury. This study also revealed a new role for ASCs in the injury response and provides insights into future strategies for ASC-based therapies.

Acknowledgments

We thank Ayako Kurata and Akiko Matsuura for technical assistance. This work was supported by Grant B2-19390452 from the Japanese Ministry of Education, Culture, Sports, Science, and Technology.

Disclosure of Potential Conflicts of Interest

The authors indicate no potential conflicts of interest.

References

1 Zuk PA, Zhu M, Ashjian P et al. Human adipose tissue is a source of multipotent stem cells. Mol Biol Cell 2002;13:4279–4295.
2 Rehman J, Traktuev D, Li J et al. Secretion of angiogenic and antiapoptotic factors by human adipose stromal cells. Circulation 2004;109:1292–1298.
3 Kilroy GE, Foster SJ, Wu X et al. Cytokine profile of human adipose-derived stem cells: Expression of angiogenic, hematopoietic, and pro-inflammatory factors. J Cell Physiol 2007;212:702–709.
4 Nakagami H, Maeda K, Morishita R et al. Novel autologous cell therapy in ischemic limb disease through growth factor secretion by cultured adipose tissue-derived stromal cells. Arterioscler Thromb Vasc Biol 2005;25:2542–2547.
5 Planat-Benard V, Silvestre JS, Cousin B et al. Plasticity of human adipose lineage cells toward endothelial cells: Physiological and therapeutic perspectives. Circulation 2004;109:656–663.
6 Miranville A, Heeschen C, Sengenes C et al. Improvement of postnatal neovascularization by human adipose tissue-derived stem cells. Circulation 2004;110:349–355.
7 Miyahara Y, Nagaya N, Kataoka M et al. Monolayered mesenchymal stem cells repair scarred myocardium after myocardial infarction. Nat Med 2006;12:459–465.
8 Rodriguez AM, Pisani D, Dechesne CA et al. Transplantation of a multipotent cell population from human adipose tissue induces dystrophin expression in the immunocompetent mdx mouse. J Exp Med 2005; 201:1397–1405.
9 Matsumoto D, Sato K, Gonda K et al. Cell-assisted lipotransfer: Supportive use of human adipose-derived cells for soft tissue augmentation with lipoinjection. Tissue Eng 2006;12:3375–3382.
10 Lendeckel S, Jodicke A, Christophis P et al. Autologous stem cells (adipose) and fibrin glue used to treat widespread traumatic calvarial defects: Case report. J Craniomaxillofac Surg 2004;32:370–373.
11 García-Olmo D, Garcia-Arranz M, Herreros D et al. A phase I clinical trial of the treatment of Crohn's fistula by adipose mesenchymal stem cell transplantation. Dis Colon Rectum 2005;48:1416–1423.
12 Yoshimura K, Sato K, Aoi N et al. Cell-assisted lipotransfer (CAL) for cosmetic breast augmentation: Supportive use of adipose-derived stem/stromal cells. Aesthetic Plast Surg 2008;32:48–55.
13 Chiou M, Xu Y, Longaker MT. Mitogenic and chondrogenic effects of fibroblast growth factor-2 in adipose-derived mesenchymal cells. Biochem Biophys Res Commun 2006;343:644–652.
14 Quarto N, Longaker MT. FGF-2 inhibits osteogenesis in mouse adipose tissue-derived stromal cells and sustains their proliferative and osteogenic potential state. Tissue Eng 2006;12:1405–1418.
15 Kakudo N, Shimotsuma A, Kusumoto K. Fibroblast growth factor-2 stimulates adipogenic differentiation of human adipose-derived stem cells. Biochem Biophys Res Commun 2007;359:239–244.
16 Kang YJ, Jeon ES, Song HY et al. Role of c-Jun N-terminal kinase in the PDGF-induced proliferation and migration of human adipose tissue-derived mesenchymal stem cells. J Cell Biochem 2005;95: 1135–1145.
17 Suga H, Shigeura T, Matsumoto D et al. Rapid expansion of human adipose-derived stromal cells preserving multipotency. Cytotherapy 2007;9:738–745.
18 Chang L, Karin M. Mammalian MAP kinase signaling cascades. Nature 2001;410:37–40.
19 Wang M, Crisostomo PR, Herring C et al. Human progenitor cells from bone marrow or adipose tissue produce VEGF, HGF, and IGF-1 in response to TNF by a p38 MAPK-dependent mechanism. Am J Physiol Regul Integr Comp Physiol 2006;291:R880–R884.
20 Aiba-Kojima E, Tsuno NH, Inoue K et al. Characterization of wound drainage fluids as a source of soluble factors associated with wound healing: Comparison with platelet-rich plasma and potential use in cell culture. Wound Repair Regen 2007;15:511–520.
21 Akita S, Akino K, Imaizumi T et al. A basic fibroblast growth factor improved the quality of skin grafting in burn patients. Burns 2005;31: 855–858.
22 Nakamura T, Mizuno S, Matsumoto K et al. Myocardial protection from ischemia/reperfusion injury by endogenous and exogenous HGF. J Clin Invest 2000;106:1511–1519.
23 Yoshimura K, Shigeura T, Matsumoto D et al. Characterization of freshly isolated and cultured cells derived from the fatty and fluid portions of liposuction aspirates. J Cell Physiol 2006;208:64–76.
24 Suga H, Matsumoto D, Inoue K et al. Numerical measurement of viable and nonviable adipocytes and other cellular components in aspirated fat tissue. Plast Reconstr Surg 2008;122:103–114.
25 Nishimura S, Manabe I, Nagasaki M et al. Adipogenesis in obesity requires close interplay between differentiating adipocytes, stromal cells, and blood vessels. Diabetes 2007;56:1517–1526.
26 Montesano R, Vassalli JD, Baird A et al. Basic fibroblast growth factor induces angiogenesis in vitro. Proc Natl Acad Sci U S A 1986;83:7297–7301.
27 Nissen NN, Polverini PJ, Gamelli RL et al. Basic fibroblast growth factor mediates angiogenic activity in early surgical wounds. Surgery 1996; 119:457–465.
28 Cordon-Cardo C, Vlodavsky I, Haimovitz-Friedman A et al. Expression of basic fibroblast growth factor in normal human tissues. Lab Invest 1990;63:832–840.
29 Schulze-Osthoff K, Risau W, Vollmer E et al. In situ detection of basic fibroblast growth factor by highly specific antibodies. Am J Pathol 1990;137:85–92.
30 Takamiya M, Saigusa K, Aoki Y. Immunohistochemical study of basic fibroblast growth factor and vascular endothelial growth factor expression for age determination of cutaneous wound. Am J Forensic Med Pathol 2002;23:264–267.
31 Muthukrishnan L, Warder E, McNeil PL. Basic fibroblast growth factor is efficiently released from a cytolsolic storage site through plasma membrane disruptions of endothelial cells. J Cell Physiol 1991;148:1–16.
32 Bashkin P, Doctrow S, Klagsburn M et al. Basic fibroblast growth factor binds to subendothelial extracellular matrix and is released by heparitinase and heparin-like molecules. Biochemistry 1989;28:1737–1743.
33 Ishai-Michaeli R, Eldor A, Vlodavsky I. Heparanase activity expressed by platelets, neutrophils, and lymphoma cells releases active fibroblast growth factor from extracellular matrix. Cell Regul 1990;1:833–842.
34 Mori S, Matsuzaki K, Yoshida K et al. TGF-β and HGF transmit the

signals through JNK-dependent Smad2/3 phosphorylation at the linker regions. Oncogene 2004;23:7416–7429.
35 Rush S, Khan G, Bamisaiye A et al. C-jun amino-terminal kinase and mitogen activated protein kinase 1/2 mediate hepatocyte growth factor-induced migration of brain endothelial cells. Exp Cell Res 2007;313: 121–132.
36 Onimaru M, Yonemitsu Y, Tanii M et al. Fibroblast growth factor-2 gene transfer can stimulate hepatocyte growth factor expression irrespective of hypoxia-mediated downregulation in ischemic limbs. Circ Res 2002;91: 923–930.
37 Roletto F, Galvani AP, Cristiani C et al. Basic fibroblast growth factor stimulates hepatocyte growth factor/scatter factor secretion by human mesenchymal cells. J Cell Physiol 1996;166:105–111.
38 Blanquaert F, Delany AM, Canalis E. Fibroblast growth factor-2 induces hepatocytes growth factor/scatter factor expression in osteoblasts. Endocrinology 1999;140:1069–1074.
39 Matsumoto K, Okazaki H, Nakamura T. Up-regulation of hepatocyte growth factor gene expression by interleukin-1 in human skin fibroblasts. Biochem Biophys Res Commun 1992;188:235–243.
40 Takami Y, Motoki T, Yamamoto I et al. Synergistic induction of hepatocyte growth factor in human skin fibroblasts by the inflammatory cytokines interleukin-1 and interferon-γ. Biochem Biophys Res Commun 2005;327:212–217.
41 Wu YL, Gohda E, Iwao M et al. Stimulation of hepatocyte growth factor production by ascorbic acid and its stable 2-glucoside. Growth Horm IGF Res 1998;8:421–428.
42 Coban YK, Kurutas EB, Ciralik H. Ischemia-reperfusion injury of adipofascial tissue: An experimental study evaluating early histologic and biochemical alterations in rats. Mediators Inflamm 2005;2005: 304–308.
43 Zengin E, Chalajour F, Gehling UM et al. Vascular wall resident progenitor cells: A source for postnatal vasculogenesis. Development 2006; 133:1543–1551.
44 Traktuev D, Merfeld-Clauss S, Li J et al. A population of multipotent CD34-positive adipose stromal cells share pericyte and mesenchymal surface markers, reside in a periendothelial location, and stabilize endothelial networks. Circ Res 2008;102:77–85.
45 Ueki T, Kaneda Y, Tsutsui H et al. Hepatocyte growth factor gene therapy of liver cirrhosis in rats. Nat Med 1999;5:226–230.
46 Liu Y. Hepatocyte growth factor in kidney fibrosis: Therapeutic potential and mechanisms of action. Am J Physiol Renal Physiol 2004;287:F7–F16.
47 Yang J, Dai C, Liu Y. Hepatocyte growth factor suppresses renal interstitial myofibroblast activation and intercepts Smad signal transduction. Am J Pathol 2003;163:621–632.
48 Bikfalvi A, Klein S, Pintucci G et al. Biological roles of fibroblast growth factor-2. Endocr Rev 1997;18:26–45.
49 Conway K, Price P, Harding KG et al. The molecular and clinical impact of hepatocyte growth factor, its receptor, activators, and inhibitors in wound healing. Wound Repair Regen 2006;14:2–10.
50 Bell LN, Cai L, Johnstone BH et al. A central role for hepatocyte growth factor in adipose tissue angiogenesis. Am J Physiol Endocrinol Metab 2008;294:E336–E344.
51 Cai L, Johnstone BH, Cook TG et al. Suppression of hepatocyte growth factor production impairs the ability of adipose-derived stem cells to promote ischemic tissue revascularization. STEM CELLS 2007;25:3234–3243.

See www.StemCells.com for supporting information available online.

Supplemental online Figure 1.

(A) BrdU incorporation assay of human ASCs cultured with injury-associated growth factors. Human ASCs were cultured in a medium with one of the growth factors (10 ng/ml) and 2% FBS for 48 hours. FGF-2 and PDGF significantly increased BrdU-positive proliferating cells ($n = 3$, $*p < 0.05$). **(B)** Representative results of flow cytometry analysis of human ASCs cultured with injury-associated growth factors. Human ASCs were cultured with one of the growth factors (10 ng/ml) for 7 days. No significant changes in the expression of vascular endothelial markers (CD31, CD34, Flk-1, or Tie-2) were observed.

Supplemental online Figure 2.

(A) Weight of the inguinal fat pad of mice after ischemia-reperfusion injury. The samples from day 1 weighed significantly more, suggesting tissue edema ($n = 3$, $*p < 0.05$). **(B)** GPDH activity of the adipose tissue after ischemia-reperfusion injury. No significant differences were observed during the 14 days of the experiment. **(C)** Immunostainig for BrdU. BrdU-positive proliferating cells increased after injury, peaking on day 3. Scale bars = 100 µm. (D) Immunostainig for TUNEL. TUNEL-positive apoptotic cells (arrows) were observed most frequently 1 day after injury. Scale bars = 100 µm.

Supplemental online Figure 3.

(A) Immunostaining of the control tissue for CD31 (green), CD34 (red) or Hoechst 33342 (blue). CD34+/CD31− cells were observed throughout the adipose tissue especially around vessels before injury. Scale bars = 20 µm. **(B)** Living tissue image stained with BODIPY (adipocytes; yellow), lectin (endothelial cells; red), or Hoechst

33342 (nuclei; blue). Increased number of nucleated cells and capillaries were observed around small-sized adipocytes. Scale bars = 20 µm. **(C)** Immunostaining of the tissue for CD68. CD68+ macrophages were scarcely found in the adipose tissue, while their aggregation, suggesting phagocytosis, was most frequently observed 3 days after injury. Scale bar = 100 µm. **(D)** Living tissue image stained with CD34 (green), lectin (endothelial cells; red), or Hoechst 33342 (nuclei; blue). The number of CD34+/lectin– cells was smaller in the group treated with a JNK inhibitor on days 3 and 7. Scale bars = 50 µm. **(E)** Vascular density in the adipose tissue 2 weeks after injury. Vascular density was calculated by counting vessels in microphotographs that were immunostained for CD31. Scale bar = 100 µm. Adipose area decreased by fibrogenesis (Fig. 7), but the final vascular density did not change significantly after injury with or without continuous administration of the JNK inhibitor SP600125 (SP).

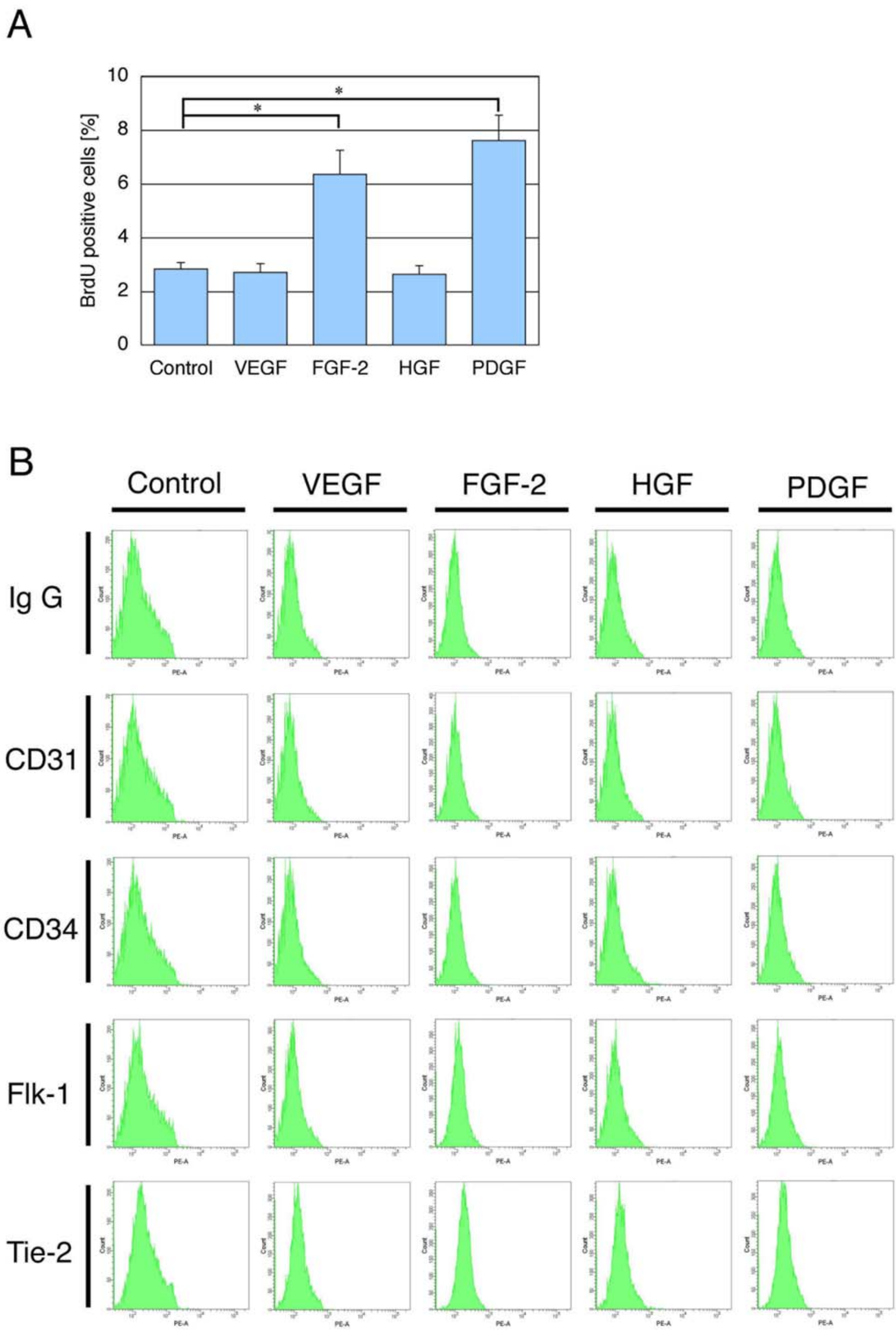
A
BrdU positive cells [%]
10
8
6
4
2
0
*
*
Control
VEGF
FGF-2
HGF
PDGF
B
Control
VEGF
FGF-2
HGF
PDGF
Ig G
CD31
CD34
Flk-1
Tie-2
Count
PE-A

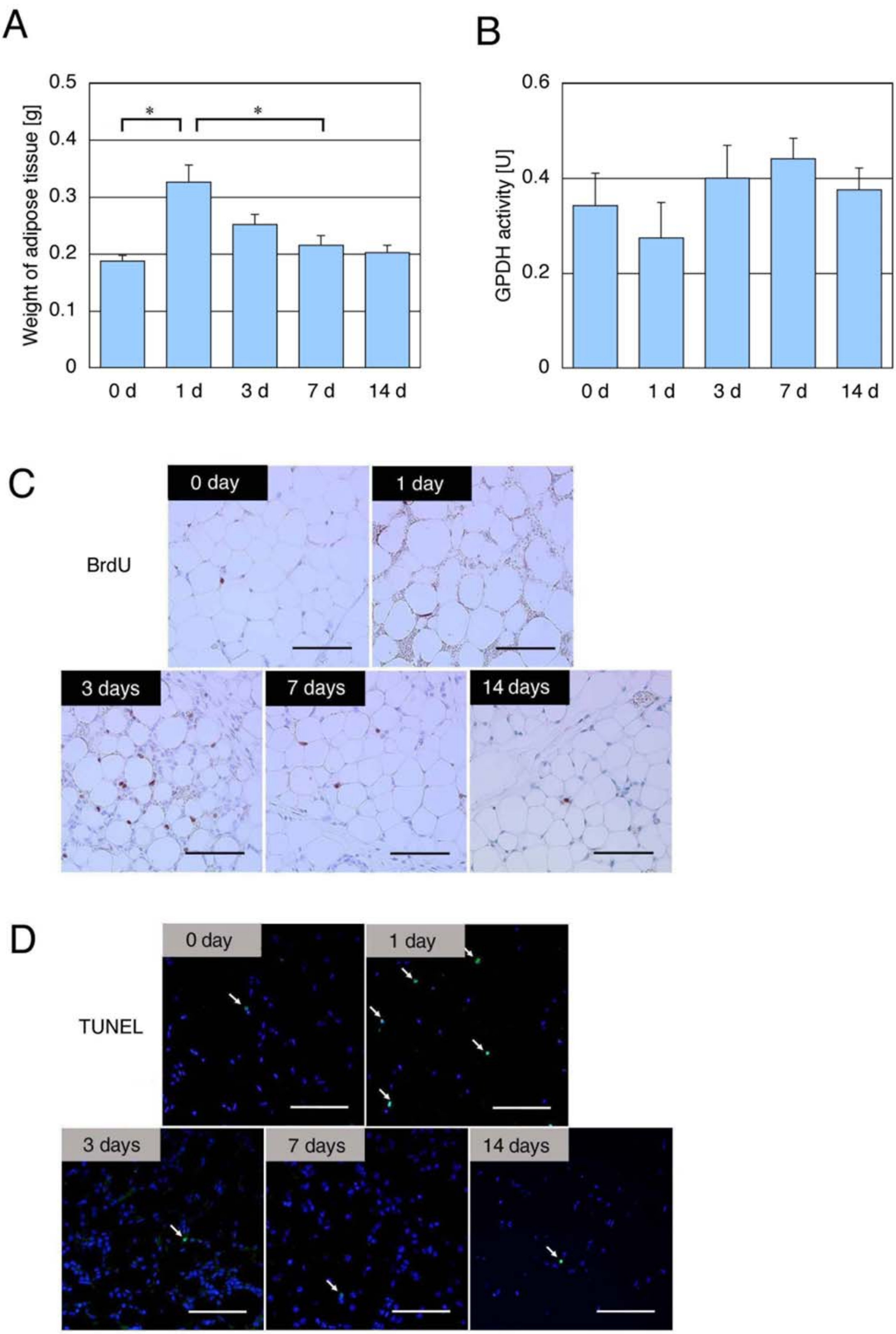
A
0.5
0.4
0.3
0.2
0.1
0
Weight of adipose tissue [g]
*
*
0 d
1 d
3 d
7 d
14 d
B
0.6
0.4
0.2
0
GPDH activity [U]
0 d
1 d
3 d
7 d
14 d
C
BrdU
0 day
1 day
3 days
7 days
14 days
D
TUNEL
0 day
1 day
3 days
7 days
14 days

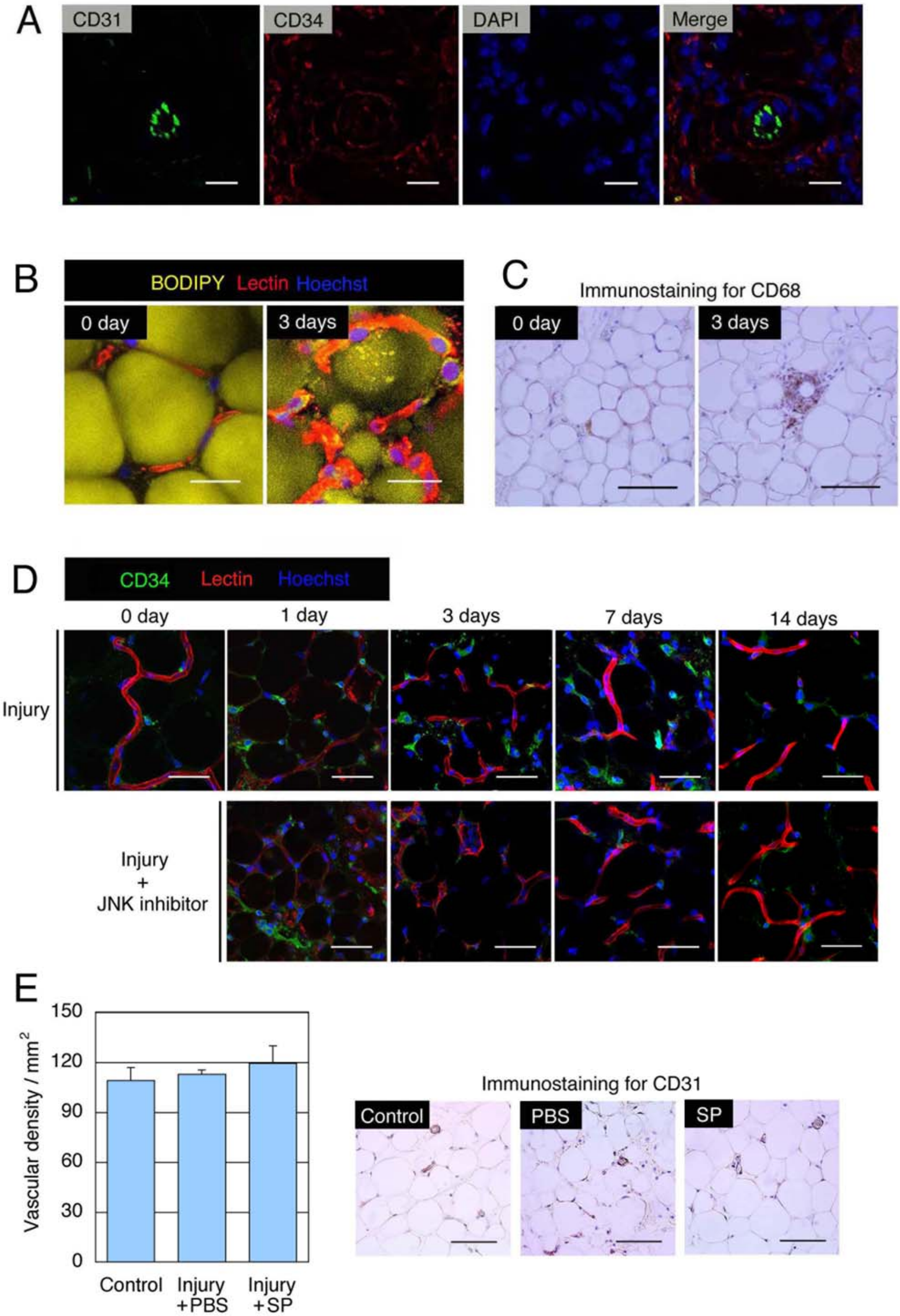
A
CD31
CD34
DAPI
Merge
B
BODIPY Lectin Hoechst
0 day
3 days
C
Immunostaining for CD68
0 day
3 days
D
CD34 Lectin Hoechst
0 day
1 day
3 days
7 days
14 days
Injury
Injury
+
JNK inhibitor
E
Vascular density / mm²
150
120
90
60
30
0
Control
Injury +PBS
Injury +SP
Immunostaining for CD31
Control
PBS
SP